Conference paper

Carolina Gambetta*, Walter A. Massad*, Andrea V. Nesci and Norman A. García

Vitamin B2-sensitized degradation of the multifunctional drug Evernyl, in the presence of visible light – microbiological implications

DOI 10.1515/pac-2015-0407

Abstract: Taking into consideration the importance of the photooxidative effects in complex bio-environments, this paper reports on the visible-light-promoted interactions between Evernyl (methyl 2, 4-dihydroxy-3,6-dimethylbenzoate, Ev) and vitamin B2 (riboflavin, Rf). Ev is a phenolic derivative, transparent to visible light, that possesses important antimicrobial activity. This compound is the first known natural, complete and specific human androgen receptor antagonist. Ev is profusely employed in personal-care products and synthesized as a secondary metabolite by several lichen and plant species. In both sceneries, acting Ev as a cosmetic component for topic applications or as a lichen constituent, may Rf behave as a native visible-light absorber pigment. In this context, kinetic and mechanistic aspects of the Rf-sensitized photooxidation of Ev, has been studied in aqueous solution, irradiating with blue LED light (463–471 nm) and employing stationary and time resolved methods. Results indicate that Ev reacts with the photogenerated reactive oxygen species (ROS) singlet molecular oxygen with a rate constant of $k_r = 1.1 \pm 0.2 \times 10^6\ M^{-1}\,s^{-1}$. In parallel Ev also quenches the electronically excited singlet and triplet excited states of Rf with rate constants close to the difussion limit. As a result the ROS superoxide radical anion and hydrogen peroxide are generated and the latter subsequently reacts with Ev. Possible implications of these photoreactions on the antimicrobial activity of Ev have been investigated employing a *Candida albicans* (CA) strain, isolated from human skin infection. The simultaneous presence of Rf, Ev in a sub-MIC, and blue-light irradiation produced a significant antimycotic effect, attributed to ROS photogeneration.

Keywords: *Candida albicans*; Evernyl; kinetics; Photobiology-16; photochemistry; riboflavin.

Introduction

Evernyl (methyl 2,4-dihydroxy-3,6-dimethylbenzoate, Ev, Scheme 1), is a naturally occurring phenolic compound. It is present in the lichen species *Evernia prunastri var. prunastri* (L.) and *Pseudevernia furfuracea* (*L.*) [1, 2]. Ev has been also isolated from higher plants like *Newbouldia laevis*, *Alseodaphne andersonii*, *Acer*

Article note: A collection of invited papers based on presentations at the 16th International Congress on Photobiology (ICP-16), Córdaba, Argentina, 7–12 September 2014. Other papers from this meeting are published in Photochemical and Photobiological Sciences and Photochemistry and Photobiology.

***Corresponding authors: Carolina Gambetta and Walter A. Massad,** Departamento de Química, Universidad Nacional de Río Cuarto, 5800, Río Cuarto, Argentina, e-mail: cgambetta@exa.unrc.edu.ar (C. Gambetta), wmassad@exa.unrc.edu.ar (W. A. Massad)
Andrea V. Nesci: Departamento de Microbiología e Inmunología, Universidad Nacional de Río Cuarto, 5800, Río Cuarto, Argentina
Norman A. García: Departamento de Química, Universidad Nacional de Río Cuarto, 5800, Río Cuarto, Argentina

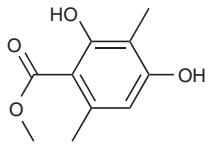

Scheme 1: Chemical structure of Evernyl (Ev).

nikense and *Frullania brasiliensis* [3–6] and identified as a degradation product of various natural depsides [7]. It has been recently shown that Ev is the first known natural, complete and specific human androgen receptor antagonist. Thus it was immediately used in benign prostate hyperplasia and prostate cancer therapies [8–10].

Ev extracted from synthetic or natural sources is widely employed in a variety of body lotions, perfumes, makeups and sunscreens [2, 11]. The phenolic derivative is responsible for the characteristic aroma of the fragrance oakmoss. Hence, it is now being used to replace oakmoss because this lichen extract was reported to cause photoallergy and photocontact-dermatitis in sensitive people [12]. Within this framework, the effect of environmental light on Ev constitutes a remarkable research matter.

Ev is transparent to visible light. Nevertheless, it must not be excluded the possibility that, during topical application, the drug could be degraded by the action of visible-light-absorber sensitizers present in human skin such as riboflavin (Rf, vitamin B2) [1]. Besides, Ev is synthesized as a secondary metabolite by several lichen and plant species [2], a natural scenery where Rf may play an in vivo photosensitizing role. The vitamin, broadly distributed in nature, and endogenously present in commercial formulations of personal care products, has been profusely reported as responsible for the photodegradation of compounds with biological and medicinal interest [3–6]. In this context, the main aim of the present research work was the elucidation of kinetic and mechanistic aspects of the potential degradation of Ev through a Rf-photosensitized process.

It has been reported that different extracts of lichens and vegetable bark containing Ev possess an important antimicrobial activity [7, 8, 11, 12]. On this basis we decided to evaluate the extent of the in vitro antifungal activity of Ev before and after blue light irradiation in the presence of vitamin B2. A *Candida albicans* (CA) strain, isolated from a human skin infection, was employed in the microbiological experiments. This yeast constitutes a common mucous membrane and skin opportunistic pathogen [9, 10, 13, 14].

Materials and methods

Materials

Evernyl, riboflavin, deuterium oxide 99.9 % (D_2O), superoxide dismutase (SOD) from bovine erythrocytes, catalase (CAT) from bovine liver, Rose Bengal (RB), furfuryl acetate (FAc) and furfuryl alcohol (FFA) were purchased from Sigma-Aldrich (MO, USA). Hydrogen peroxide (H_2O_2), 100 vol. was obtained from Parsol (Argentina). Ascorbic acid [(R)-3,4-dihydroxy-5-((S)-1,2-dihydroxyethyl)furan-2(5H)-one, Asa] was from Cicarelli (Argentina). Sabouraud dextrose agar medium was purchased from Laboratorios Britania S.A (Argentina). All these chemicals and the culture medium were used as received. Water was triply distilled. All the measurements were carried out at room temperature employing freshly prepared solutions. The working pH was 7 ± 0.1, employing phosphate buffer.

Absorption and fluorescence measurements

Ground state absorption spectra were registered employing a Hewlett Packard 8453 diode array spectrophotometer.

Steady-state fluorescence was measured with a Spex Fluoromax spectrofluorometer at 25 ± 1 °C in air-equilibrated solutions and fluorescence lifetimes were determined by a time-correlated single photon counting technique (SPC) on an Edinburgh FL-900CD instrument, equipped with a blue LED (PicoQuant PLS 450). Excitation and emission wavelengths for Rf were 450 and 515 nm, respectively.

The rate constants for interactions of the excited singlet state of the Rf (^{1}Rf*) with Ev were determined employing a classical Stern–Volmer treatment of the data (eqs. 1 and 2).

$$I_0 / I = 1 + K_{SV}[\text{Ev}] \quad \text{eq. (1)}$$

$$^1\tau_0 / {}^1\tau = 1 + {}^1K_Q {}^1\tau_0 [\text{Ev}] \quad \text{eq. (2)}$$

Where I, I_0, $^1\tau$ and $^1\tau_0$ are the respective steady-state intensities and lifetimes for Rf fluorescence in the presence and in the absence of Ev, being $K_Q = {}^1k_q {}^1\tau_0$

Stationary photolysis

Stationary aerobic photolysis of aqueous solutions containing Ev and Rf was carried out in a homemade photolyzer, using blue (λ_{max} = 467 nm) or green (λ_{max} = 510 nm) LEDs as photoirradiation sources, for Rf- and RB-sensitization, respectively.

Oxygen uptake experiments

The steady state aerobic photolysis of aqueous solutions containing Ev and Rf was carried out in a homemade photolyser provided with a 150 W quartz-halogen lamp. A cut-off filter of 400 nm was used to select the irradiation wavelengths. Oxygen uptake in water was monitored with a polarographic 97-08 Orion electrode.

Kinetic measurements

The reactive rate constant for the chemical reaction of $O_2(^1\Delta_g)$ with Ev (k_r) was determined using a relative method (eq. 3), for which the knowledge of the reactive rate constant for the photo-oxidation of a reference compound R is required:

$$\text{slope} / \text{slope}_R = k_r / k_{rR} \quad \text{eq. (3)}$$

where slope and slope$_R$ are the respective slopes of the first-order plots of Ev and reference consumption. The reference compound was FAc, with a reported k_r value of 5.5×10^7 M^{-1} s^{-1} [15].

The total quenching rate constant for $O_2(^1\Delta_g)$ deactivation by Ev (k_t), was determined employing the already described time-resolved phosphorescence detection (TRPD) equipment [5]. Usually, 15 shots were needed for averaging so as to achieve a good signal-to-noise ratio, from which the temporal decay curve was obtained. Air equilibrated solutions were employed in all cases.

$O_2(^1\Delta_g)$ lifetimes were evaluated in the presence (τ) and in the absence (τ_0) of Ev and the data was plotted as a function of quencher concentration, according to a simple Stern–Volmer treatment (eq. 4).

$$1/\tau = 1/\tau_0 + k_t[\text{Ev}] \quad \text{eq. (4)}$$

D_2O was employed as a solvent in the TRPD experiments, in order to enlarge the phosphorescence lifetime of $O_2(^1\Delta_g)$ within temporal range attainable by our photodetector [16].

The evaluation of Ev photostability was performed employing Asa as a reference compound. The experiments were made employing 0.04 mM Rf as a sensitizer, in pH 7 buffer, under blue-light irradiation. Absorbance changes for both substrates were monitored at 266 nm.

The thermally-driven experiments on the reaction H_2O_2 + Ev were performed by adding the adequate amount of a solution of 100 vol H_2O_2 to 2 mL aqueous solution of 0.25 mM Ev contained in a spectrophotometric cell, under constant magnetic stirring. The absorbance changes at 266 nm were continuously monitored and plotted vs. time elapsed after mixing.

Laser flash photolysis experiments

Transient absorption spectra were determined in Argon-saturated 0.04 mM Rf aqueous solutions using a flash photolysis apparatus provided with a 150 W Xenon lamp as analyzing light. A 355 nm Nd:YAG laser output was employed as excitation source. The detection system comprised a PTI monochromator and a red-extended photomultiplier (Hamamatsu R666). The signal, acquired and averaged by a digital oscilloscope (Hewlett-Packard 54504A), was transferred to a PC *via* an HPIB parallel interface, where it was analyzed and stored. ^{3}Rf* disappearance was monitored from the first-order decay of the absorbance at 670 nm, which is a zone where the interference of other species is negligible. To avoid self-quenching and triplet-triplet annihilation, ^{3}Rf* decay was measured at low concentrations of the vitamin (typically 0.05 mM) and low enough laser energy.

For the determination of the rate constant for interaction of ^{3}Rf*–Ev (^3k_q), the Stern–Volmer expression shown in eq. 5 was employed.

$$1/^3\tau = (1/^3\tau_0) + {}^3k_q[\mathrm{Ev}] \qquad \text{eq. (5)}$$

Where $^3\tau$ and $^3\tau_0$ are the experimentally determined lifetimes of ^{3}Rf* in the presence and in the absence of Ev.

To perform the transient absorption spectra, the signals were fitted at each wavelength employing a bi-exponential decay function. The lifetime values were shared in the global fit using origin 8.0 (Originlab Corp., Northampton, MA, USA) software. The spectra were obtained by plotting the pre-exponential factors (a_i) for each lifetime using eq. 6 with i = 2 [17, 18]:

$$\Delta A(t) = a_0 + \sum_i a_i e^{(-t/\tau_i)} \qquad \text{eq. (6)}$$

Viability experiments on *Candida albicans*

Yeast strain and culture conditions: CA strain was obtained from a human skin clinical infection. The fungal strain was maintained in a Sabouraud dextrose agar Petri dish (Britania, Buenos Aires, Argentina) at 2 °C for the time that the experiment lasted. In order to achieve a standard amount of approximately 10^8 cells/mL the strain was cultured overnight in Sabouraud dextrose broth (Britania, Buenos Aires, Argentina) in orbital agitation at 37 °C. Quantification of cells was performed both by Neubauer chamber counting and viable cell counting on the Petri dish surface.

Photosensitizer: Rf was used as sensitizer. The appropriate volume to achieve an absorbance of 0.3 at 445 nm in the test tube was added by filtration (0.2 μm filter, Merk Millipore, Darmstadt, Germany).

Ev stock solution: The Ev ethanolic solution was added to vials tubes in a concentration of 250 ppm, to maintain Ev concentration below the MIC (300 ppm), which was previously determined (data not shown).

Irradiation source: a LED light array system (FOG Electrónica, Argentina) was constructed using 32 LED units (3.3 V, 20 mA each one) that emitted blue light (λ = 463–471 nm). An laser power meter (UNO, Gentec-Eo) was used to determine the LED irradiance at 465 nm. A value of 47.8 μW/cm^2 was measured for each blue LED. The light array was disinfected previously to each irradiation test using ethanol–water solution (70 % v/v).

Effect of Ev and Rf on the viability of CA after blue LED light irradiation: to investigate the in vitro antimicrobial effects of blue light, Rf and Ev, alone and combined, on CA assays were performed in triplicate. A 100 μL aliquot of the overnight inoculum dilution (10^3 CFU/mL) was placed inside sterile vials tubes containing 2.5 mL of sterile distilled water. One vial tube was used per each treatment. The fungal viability after treatment was assessed by viable cell counting using Petri plate surface method. Sabouraud dextrose agar was used as culture medium. CFU/mL were counted after 24 h of incubation at 37 °C in dark.

Table 1: Treatments used as comparative parameters for in vitro assays and descriptive results on *Candida albicans* viavility.

Run	Description	Viability inhibition
Control 1: Blank L – Rf – Ev–	Yeast cells inoculated in the dark, without addition of Rf or Ev.	No inhibition after 30 min
Control 2: L + Rf – Ev–	Yeast cells exposed to light without addition of Rf or Ev.	*ca.* 65 % inhibition[a, b]
Treatment 1: L + Rf + Ev–	0.03 mM Rf added. Fungal viability assessed after light exposure.	*ca.* 67 % inhibition[a, b]
Treatment 2: L + Rf – Ev+	250 ppm Ev added. Fungal viability assessed after light exposure.	*ca.* 74 % inhibition[a, b]
Treatment 3: L + Rf + Ev+	0.03 mM Rf + 250 ppm Ev added. Fungal viability assessed after light exposure.	*ca.* 95 % inhibition[a]

[a]After 30 min blue light-exposure; [b]No statistically different results.

In order to compare the antifungal effects of blue light, Ev and Rf, five treatments were performed as shown in Table 1. Each treatment was assayed in triplicate.

Statistical treatment of data: statistical analysis of the experimental data was performed using one-way analysis of variance (ANOVA) and Origin 8.0 software (Originlab Corp., Northampton, MA, USA). All results showed homogeneity of variance. Mean comparisons were carried out with the Tukey test, which retains the overall significance level at 5 % ($p < 0.05$) [19].

Results

The self-explanatory Scheme 2 on Rf-photosensitization, in the presence of an electron-donating species represented by Ev in this work, was employed for presentation and discussion of the results. A similar reaction scheme has been used for these purposes by different authors [20–22].

Dark complexation Rf-Ev and interaction ^{1}Rf*-Ev

The absorption spectrum of Rf vs Rf + Ev shows the presence of a new band at 426 nm, evident in Fig. 1 (inset). Considering that no absorption from Ev is expected over 350 nm, the species absorbing in this region should be ascribed to the Rf-Ev dark complex [process (1)], being K_{ass} the complex association constant.

$$\mathrm{Rf} + \mathrm{Ev} \underset{K_{ass}}{\rightleftharpoons} [\mathrm{Rf} \cdots \mathrm{Ev}] \quad (1)$$

Rf presents a fluorescence emission band centered at 515 nm, with a reported fluorescence quantum yield (Φ_F) of 0.25 [3]. In the presence of Ev, the fluorescence quenching ^{1}Rf* produces a decrease in the steady

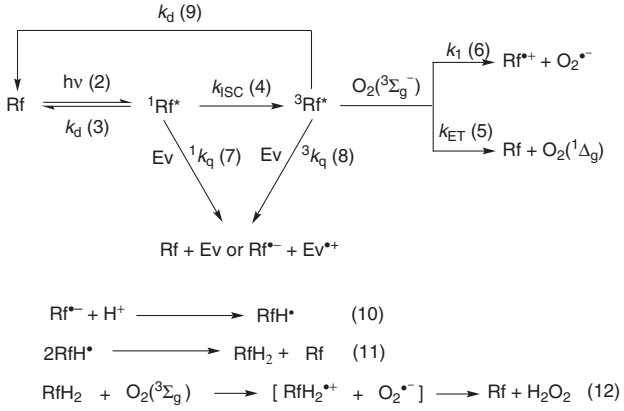

Scheme 2: Possible reactions in the visible light irradiation of riboflavin (Rf) in the presence of Evernyl (Ev).

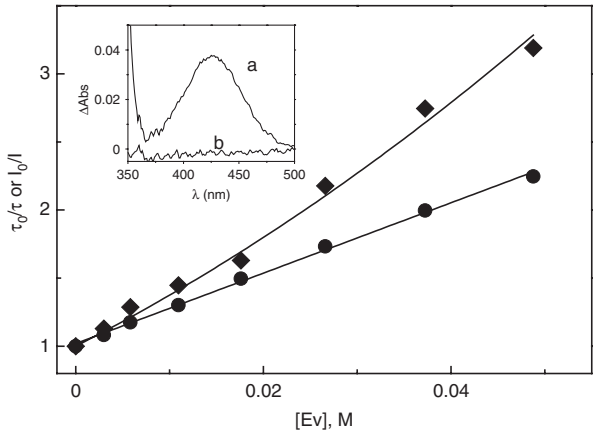

Fig. 1: Stern–Volmer plots for the steady state (◆) and time-resolved (●) fluorescence quenching of ^{1}Rf* by Ev. Inset: (a) Absorption spectrum of 0.031 mM Rf + 0.025 M Ev in water; (b) baseline.

state emission intensity without change in shape of the fluorescence spectrum. The Stern–Volmer plots obtained from these measurements presents a neat positive curvature, typical for cases in which a fluorescent species is simultaneously affected by dark association in its ground state and by collisional quenching of its excited singlet state (Fig. 1) [5, 23]. The dynamic contribution was evaluated by SPC technique, obtaining a value of $^1k_q = 4.5 \times 10^9\ M^{-1}\ s^{-1}$ [process (7), scheme 2]. The apparent association constant value for the system, was derived from the modified Stern–Volmer equation $I_0/I = (1 + K_D[Q])(1 + K_{ass}[Q])$ [5, 23], where $K_D = {}^1k_q\ {}^1\tau_0$ accounts for the dynamic component of the fluorescence quenching, being $^1\tau_0$ the ^{1}Rf* lifetime. K_D was calculated from time-resolved measurements, with $^1\tau_0 = 5.62$ ns. A value of $K_{ass} = 9.3 \pm 0.5$ was obtained by non-linear least square fitting employing the mentioned modified Stern–Volmer equation.

Photoirradiation of the mixture Rf plus Ev with visible light

The blue-light irradiation of the mixture 0.041 mM Rf + 0.033 mM Ev in water produces the spectral changes shown in Fig. 2. In parallel oxygen uptake was observed, upon photoirradiation of a similar mixture [curve (a) Fig. 2, inset]. These results, not observable in the absence of light and oxygen, strongly suggest transformations in both Rf and Ev with participation of electronically excited states of the vitamin, already detected for

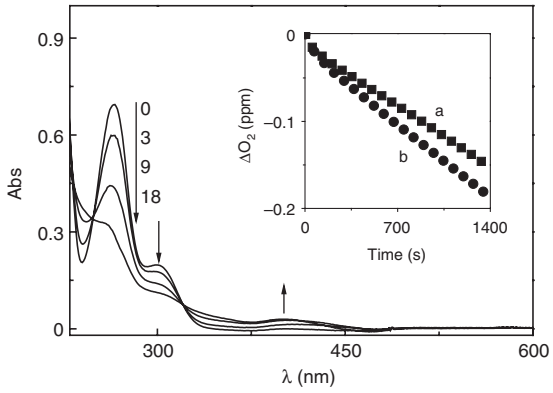

Fig. 2: Absorption spectra of aqueous solutions 0.041 mM Rf + 0.3 mM Ev vs. 0.041 mM Rf upon irradiation, under air-saturated conditions. Numbers on the spectra represent irradiation time in minutes. Inset: Oxygen uptake as a function of blue-light photoirradiation time of aqueous solutions containing: (a) 0.047 mM + 0.25 mM Ev and (b) + 20 nM SOD.

^{1}Rf*. Additionally should be taken into account the possible contribution of ROS such as $O_2(^1\Delta_g)$ (processes 5) and/or $O_2^{\bullet-}$ (processes 6) generated from ^{3}Rf* which are produced with quantum yields of 0.49 and 0.009, respectively [24].

Laser flash photolysis experiments. Quenching of ^{3}Rf* by Ev

In order to investigate the possible involvement ^{3}Rf* in the Rf-photosensitized degradation of Ev, laser flash photolysis experiments were performed.

The transient absorption spectrum of the Rf solution was fitted to eq. 6 employing the lifetime values τ_1 = 14.6 μs and τ_2 = 184 μs. From the global fit, the decay-associated spectrum after Rf excitation for τ_1 is coincident with that attributed to ^{3}Rf* [profile (a) in Fig. 3] [25–27], while the associated spectrum for τ_2 is similar to that reported to account for the species RfH$^\bullet$ [profile (b) in Fig. 3] [28, 29]. Subsequently, the transient absorption spectrum of a solution of Rf, but now in the presence of 0.3 mM Ev was fitted to eq. 6 with two lifetimes. An increase in the absorption of the species RfH$^\bullet$ was observed, with τ_2 = 148 μs [profile (c) in Fig. 3], whereas the absorption corresponding to ^{3}Rf* (with τ_1 = 2.9 μs), totally overlaps with that obtained for ^{3}Rf* in the absence of Ev [profile (d) in Fig. 3]. From these results, the transient Rf spectra determined in the absence in the presence of Ev, clearly represent the species ^{3}Rf* and RfH$^\bullet$. The latter is formed after an electron transfer process [step (8)] to yield the radical Rf$^{\bullet-}$, rapidly protonated to the neutral radical RfH$^\bullet$, a species for which a pK_a = 8.3 has been reported [process (10)] [28, 29].

A systematic reduction of ^{3}Rf* lifetime was observed in the presence of increasing concentrations of Ev, supporting the occurrence of reaction (8) between the cosmetic-additive and ^{3}Rf*, for which a rate constant value $^3k_q = 6.2 \pm 0.3 \times 10^9$ M^{-1} s^{-1} was graphically determined as shown in Fig. 3, inset.

Involvement of $O_2(^1\Delta_g)$ in Ev photodegradation. Determination of k_t and k_r

The possible involvement of $O_2(^1\Delta_g)$ in Ev photodegradation was investigated employing the exclusive $O_2(^1\Delta_g)$-generator RB. This xanthenic dye generates the oxidative species with a quantum yield of 0.75 in water [30]. Rf was not used in this kinetic determination in order to avoid possible interferences by other oxidative species produced by the vitamin.

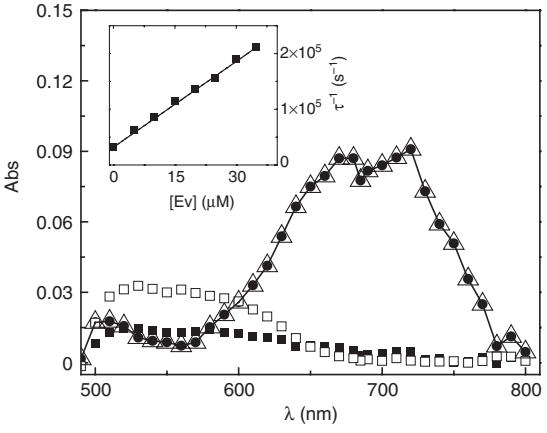

Fig. 3: Decay-associated spectra after excitation of 40 μM Rf in Ar-saturated aqueous solution in the absence and in the presence of 0.3 mM Ev. The spectra were calculated by globally fitting all the individual-wavelength data using eq. 6 (see experimental section) with two lifetime values. Rf solution: (●) τ_1 = 14.6 μs; (■) τ_2 = 184 μs. Rf + Ev solution: (Δ) τ_1 = 12.9 μs; (□) τ_2 = 148 μs. **Inset:** Stern–Volmer plot for the quenching of ^{3}Rf* by Ev.

Photoirradiation of the mixture of RB [$A(549) = 0.4$] + 0.033 mM Ev in water, generates spectral changes, shown in Fig. 4, in principle attributable to a $O_2(^1\Delta_g)$-mediated chemical transformation of Ev as described by reactions (13)–(17).

$$RB + h\nu \rightarrow {}^1RB^{\star} \tag{13}$$

$${}^1RB^{\star} \xrightarrow{k_{ISC}} {}^3RB^{\star} \tag{14}$$

$${}^3RB^{\star} + O_2({}^3\Sigma_g^-) \rightarrow RB + O_2({}^1\Delta_g) \tag{15}$$

$$O_2\left({}^1\Delta_g\right) + Ev \xrightarrow{k_r} Prod16 \tag{16}$$

$$O_2\left({}^1\Delta_g\right) + Ev \xrightarrow{kq} O_2({}^3\Sigma_g^-) + Ev \tag{17}$$

Being $k_q + k_r = k_t$

The presence of Ev in the sub-mM concentration range quenches the IR phosphorescence emission of $O_2(^1\Delta_g)$, as detected by TRPD. These experiments clearly demonstrates the existence of the interaction $O_2(^1\Delta_g)$-Ev, which may be physical in nature [process (17)] and/or reactive [process (16)]. The overall quenching constant value of $k_t = (3.6 \pm 0.3)\ 10^6\ M^{-1}\,s^{-1}$ was obtained for Ev (Fig. 4, Inset A). In parallel a value of $(1.1 \pm 0.2) \times 10^6\ M^{-1}\,s^{-1}$ was determined for the reactive rate constant k_r, employing the actinometric method described in the experimental section (Fig. 4, Inset B).

The possible role of the ROS $O_2^{\bullet-}$ and H_2O_2 in the Rf-sensitized oxidation of Ev

The rate of oxygen consumption by a photoirradiated solution of 0.040 mM Rf + 0.25 mM Ev was increased when performed in the presence of 20 nM SOD, as shown in Fig. 2 (inset). The enzyme specifically produces the dismutation of the species $O_2^{\bullet-}$ through process (18) [31].

$$2H^+ + 2O_2^{\bullet-} \rightarrow H_2O_2 + O_2 \tag{18}$$

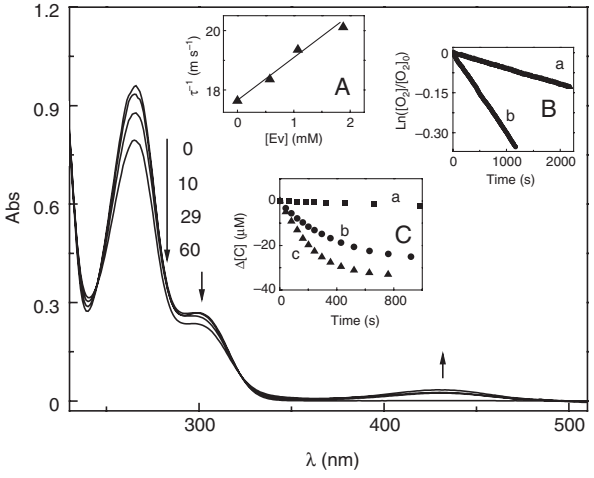

Fig. 4: Absorption spectra of aqueous RB ($A(549) = 0.4$) + 0.3 mM Ev vs. RB [$A(549) = 0.4$] upon photoirradiation at 510 nm under air-saturated conditions. Numbers on the spectra represent irradiation time in minutes. Inset A: Stern–Volmer plot for the quenchingof $O_2(^1\Delta_g)$ phosphorescence by Ev. Inset B: First order plot for oxygen uptake by aqueous solutions of RB ($Abs_{549} = 0.4$) plus 0.3 mM Ev (a) and 0.3 mM FFA (b), upon visiblelight irradiation (cut-off 400 nm). Inset C: Changes in the molar concentration of individual solutions of 0.35 mM Asa (c), and 0.35 mM Ev (b) as a function of blue-light-irradiation time in the presence of 0.04 mM riboflavin as a sensitizer, in pH 7 buffered aqueous solution. Trace (a) corresponds to changes in molar concentration of the sensitizer solution in the absence of additives. Monitoring wavelength: 265 nm.

The increase in the rate of oxygen uptake induced by the presence of the enzime supports the mechanistic involvement of the species $O_2^{\bullet-}$, as stated in Scheme 2. Nevertheless, a neat decrease in that rate should be expected for cases in which $O_2^{\bullet-}$ were the prevailing oxidative species, according to reaction (19).

$$Ev + O_2^{\bullet-} \rightarrow Prod\,19 \tag{19}$$

It is well known that in $O_2^{\bullet-}$-mediated mechanism, SOD can either preclude or stimulate the oxidation of a given substrate, depending on the particular mechanistic role. That is, the ultimate effect will depend on whether the ROS acts either as a final oxidative species or as an intermediate in the subsequent generation of other ROS [32].

It has been reported that the presence of SOD favors the H_2O_2-mediated oxidation of a series of biologically-relevant hydroxyl-aromatic derivatives including gallic acid and hydroquinones [32]. A similar behavior, through reaction (20), can be assumed in the case of the phenolic compound Ev,

$$H_2O_2 + Ev \rightarrow Prod\,20 \tag{20}$$

In order to assess this possibility, the photolysis of the mixture 0.043 Mm Rf + 0.25 mM Ev in the absence and in the presence of 0.04 and 0.4 nM CAT was performed. H_2O_2 is decomposed by CAT according to reaction (21).

$$2H_2O_2 + CAT \rightarrow 2H_2O + O_2(^3\Sigma_g^-) \tag{21}$$

Spectral changes of the photolyzed solution, monitored at 266 nm and similar to those shown in Fig. 2, experimented a decrease in the Ev decomposition rate as CAT concentration increased. This result, shown in Fig. 5, strongly suggests the involvement of H_2O_2 in the Rf-sensitized photodegradation of Ev.

The viability of the reaction of H_2O_2 + Ev was tested through a simple thermally-driven assay, by plotting the 266 nm-spectral decrease of the Ev absorption band as a function of time elapsed after the mixture H_2O_2-Ev. The decomposition rate of Ev rises with the increase of H_2O_2 concentration, as show in Fig. 5, inset.

It is important to note that the individual presence of SOD and CAT, dissolved in a D_2O solution in similar conditions as employed in the described auxiliary $O_2^{\bullet-}$ and H_2O_2 tests, did not change the lifetime of $O_2(^1\Delta_g)$. It was evaluated through TRPD using RB [A(549) = 0.4] as a photogenerator of the ROS.

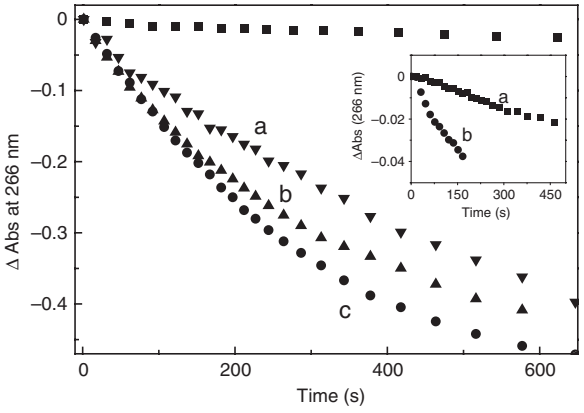

Fig. 5: The effect of CAT on the photosensitized oxidation of Ev at 266 nm for the visible-light irradiation of aqueous solutions containing: (■) 36 μM Rf; 36 μM Rf + 0.25 mM Ev and CAT: (●) 0 mM, (▲) 0.04 nM and (▼) 0.4 nM. Inset: Changes in Abs at 266 nm for the reaction of 0.25 mM Ev and H_2O_2: (■) 3.6 mM and (●) 18 mM.

Evaluation of Ev photostability against ascorbic acid as a reference compound

So far, experimental evidence clearly indicates that Ev is photooxidized in aqueous solution through a Rf-photosensitized process, with participation of ROS. Nevertheless, this result is some vague in photostability terms. Since several reactive species are simultaneously involved in Ev photodegradation, it is interesting to establish a comparative standard for the whole oxidative event. Hence, in order to perform a quantitative evaluation in relative terms, the overall photodecomposition rates of Ev and Asa were evaluated. Asa, transparent to visible light and currently known as vitamin C, is probably the most extensively studied biologically-relevant substrate in relation to Rf-photosensitized degradations. This pathway has been suggested as the main cause for the in-vivo photodegradation of vitamin C [21, 33–36].

Aqueous solutions of Rf as a sensitizer in the presence of identical concentrations of Ev and Asa were individually photolized with blue-light. The respective molar degradation rates ($Rate_{Ev}$ and $Rate_{Asa}$), were evaluated from the initial slopes of the degradation profiles represented in inset C of Fig. 4. Results indicate a ratio $Rate_{Asa}/Rate_{Ev} \sim 2$.

Effects of Ev, blue light and Rf on CA viability

A resume of results on control runs and treatments for the in vitro assays of CA viability in the presence of different combinations of blue-light, Rf and Ev are shown in Table 1.

No inhibitory effect on the strain of CA yeast cell viability was observed when 0.03 mM Rf was added in the dark to the culture medium, in accord with previous reports [37–39]. In parallel, a MIC of 300 ppm Ev was determined for the CA strain. This result is in agreement with previous studies on compounds possessing a phenolic OH attached to the aromatic ring and able to inhibit the growth of the CA strain. [40] Hence, a concentration of 250 ppm was employed in the present series of experimental assays.

Control runs on CA strain viavility (Control 2, Table 1) were performed employing only blue-light irradiation. Results show a decrease in the strain viability with irradiation time (Fig. 6). Statistically similar results

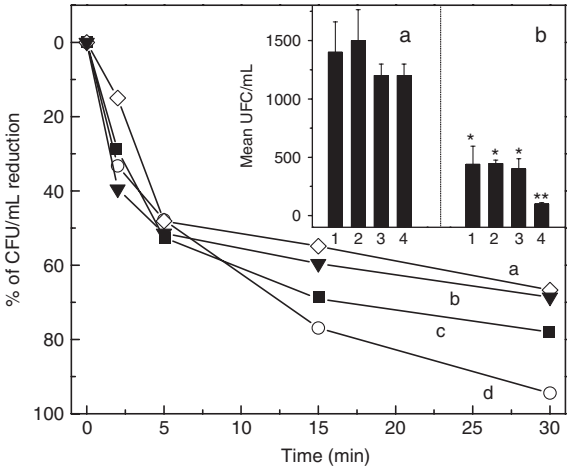

Fig. 6: Percentage of *Candida albicans* reduction in CFU/mL vs. Blue- lirradiation time in different treatments. (a): cellular suspension + light irradiation (L+ Rf- Ev-). (b): Celular suspension + light irradiation + 250 ppm Ev (L + Rf – Ev+). (c): Celular suspension + light irradiation + 0.026 mM Rf (L + Rf + Ev–). (d): Celular suspension + light irradiation + 250 ppm Ev + 0.026 mM Rf (L + Rf + Ev+). Inset: Means of *Candida albicans* CFU/mL. A: without irradiation and B: after 30 min of blue-light irradiation. **1**: L + Rf – Ev–, **2**: L + Rf + Ev–, **3**: L + Rf – Ev+ and **4**: L + Rf + Ev+. A different symbol, either * or ** indicates significant differences according to the Tukey test ($p < 0.05$). Error bars represent standard deviations.

–according to Tukey test ($p < 0.05$)– were obtained for 0.03 mM Rf without Ev and 0.03 mM Rf with Ev added (treatments 1 and 2 in Fig. 6 and Table 1).

The higher reduction in CA viavility (*ca*. 95 % after 30 min light irradiation), statitically different from run control 2 and treatments 1 and 2 occurred with treatment 3 (Table 1), it is in the simultaneous presence of light, Rf and Ev. In other words, even when photoirradiation in the absence and in the presence of Rf produces a moderate inhibition in cell viability of CA yeast, the addition of Ev, in a sub-MIC condition, constitutes the key factor for an significant inhibitory effect on the strain (Table 1 and Fig. 6).

Discussion

The ability of Rf to form dark complexes with different families of biologically-relevant substrates is well known [5, 6, 15, 16, 41]. Absorption and fluorescence results indicate the formation of a dark complex Rf-Ev, with an association constant $K_{ass} = 9.3\ M^{-1}$. This value denote a weak interaction and points out that the complexed fraction of the pigment is low enough to be ignored under sensitizing conditions.

The presence of Ev in different biological environments and its employment in personal care products of topical application makes of it an excellent candidate for Rf-photopromoted interactions. In this context, our present research work demonstrate, through TRPD experiments and auxiliary qualitative runs, that the Rf-sensitized photodegradation of Ev operates at least through two oxygen-consumer pathways, mediated by the ROS $O_2(^1\Delta_g)$ and H_2O_2. These results also suggest that reaction (19) implying a direct participation of $O_2^{\bullet-}$ as an oxidative agent, should not constitute a significant mechanistic step in the case of Ev.

The ROS $O_2(^1\Delta_g)$ and H_2O_2 are produced with the involvement of $^3Rf^*$. The predominance of either of the two oxidative processes, represented by reactions (16) and (20), depends in principle on the overall prevalence of steps (5) and the addition of (6) + (8), respectively. It is noteworthy that H_2O_2 is generated from $O_2^{\bullet-}$ as a precursory species and that reaction (6), with a reported quantum yield lower than 0.01, [24] has a limited contribution to that generation. In other words, the mentioned kinetic prevalence will depend on the competence between $O_2(^3\Sigma_g^-)$ [process (5)] and Ev [process (8)] by the excited species $^3Rf^*$. Considering $k_{ET} = 7 \times 10^8\ M^{-1}\,s^{-1}$ for process (5) in H_2O [42], and the obtained value $^3k_q = 6.2 \pm 0.3 \times 10^9\ M^{-1}\,s^{-1}$, it can be assumed that, for the same concentrations of Ev and dissolved $O_2(^3\Sigma_g^-)$, the rate for $RfH^\bullet$ production is *ca*. nine times higher than the corresponding one for $O_2(^1\Delta_g)$ generation.

The absolute k_t and k_r values for Ev in neutral aqueous solution are significantly lower than those corresponding to highly to moderate reactive substrates [43–45]. Nevertheless, mechanistic evidence points, in principle, to a partial contribution of a $O_2(^1\Delta_g)$-mediated process.

The efficiency of a $O_2(^1\Delta_g)$-promoted photooxidative step for a given substrate can be estimated through the evaluation of the k_r/k_t ratio, i.e. the fraction of overall quenching that in fact leads to chemical reaction. Although in the case of Ev the reactive contribution reaches a value *ca*. 30 %, the corresponding rate constant value, k_r in the order of $10^6\ M^{-1}\,s^{-1}$, still very low in relative terms. Hence, the $O_2(^1\Delta_g)$-oxidative pathway must be considered fairly modest, being the dominant role attributable to a H_2O_2-mediated mechanism.

Comparative evaluation of Ev photostability

In a recent paper we show that Asa, in the presence of Rf and visible light, participates in the generation and subsequent deactivation the ROS $O_2(^1\Delta_g)$, $O_2^{\bullet-}$, H_2O_2 and $OH^\bullet$ [36]. As in the present case for Ev, the main reactive pathway is mediated by $O_2^{\bullet-}$ production after the quenching of $^3Rf^*$ by Ev, in detriment to the $O_2(^1\Delta_g)$-mediated mechanism.

According to our results the overall rate for Rf-sensitized oxygenation of Asa is only two-fold higher than exhibited by Ev. On this basis, the latter should be also considered as a labile compound toward photoinduced oxidation.

Microbiological implications of Rf + Ev photoirradiation in the presence of CA strain

It is well known the general antimicrobial activity of Ev and its specific action against certain fungal strains [7, 8, 11, 12]. Nevertheless, it is worth to mention that after Rf-photosensitized irradiation, the antimycotic effect of this perfuming agent does not decrease; on the contrary, it shows a significant increase. In fact, more than 90 % of inhibition on CA strain viability rate was reached after the simultaneous application of Ev, Rf and blue light photoirradiation.

It has been recently reported a notorious reduction in CA viability employing only blue-light irradiation [46]. This photo-inhibitory effect, checked by ourselves in control run 2 (Table 1), is attributed to the presence of CA intracellular sensitizers such as flavins and flavoproteins, which are responsible for photopromoted intracellular generation of ROS after blue light irradiation, being CA highly susceptible to H_2O_2 [46, 47].

The observed effect on the combined action of blue light, Rf and Ev can be evaluated as an increase in *ca*. 30 % inhibitory effectiveness by comparing control run 2 and treatment 3 in Table 1. This may be due to the Ev-stimulated generation of ROS in the Rf-photosensitization, whith the consequent accumulation of H_2O_2 in the tests solutions, a process already discussed on kinetic basis in previous paragraphs.

Conclusions

Ev is photooxidized through a Rf-photosensitized process, with participation of $O_2(^1\Delta_g)$ and H_2O_2, both ROS photogenerated with the involvement of ^{3}Rf*. Kinetic analysis and mechanistic evidence points to the H_2O_2-mediated oxidation as the prevailing pathway.

The simultaneous presence of Ev in a sub-MIC, Rf and blue light produced a significant inhibitory effect on the viability of CA strain, attributable to H_2O_2 photo-accumulation in the fungal culture medium.

List of abbreviations

Asa Ascorbic acid
CA *Candida albicans*
CAT catalase
CFU colony forming units
D_2O Deuterium oxide
Ev Evernyl
FAc Furfuryl acetate
FFA Furfuryl alcohol
L – Rf – Ev– Absence of all three components: Light, Rf and Ev
L + Rf – Ev– Photoirradiation in the absence of Rf and Ev
L + Rf + Ev– Photoirradiation in the presence of Rf and in the absence of Ev
L + Rf – Ev+ Photoirradiation in the absence of Rf and in the presence of Ev
L + Rf + Ev+ Photoirradiation in the presence of Rf and Ev
LED Light emitting diode
MIC Minimum inhibitory concentration
$O_2(^1\Delta_g)$ Singlet molecular oxygen
$O_2^{\bullet-}$ Superoxide radical anion
$OH^{\bullet}$ hydroxyl radical
RB Rose Bengal
Rf Riboflavin (vitamin B2)
^{1}Rf* excited singlet state of the Rf
^{3}Rf* excited triplet state of the Rf
ROS Reactive oxygen species
SOD Superoxide dismutase
SPC Time-correlated single photon counting
TRPD Time-resolved phosphorescence detection

Acknowledgments: Financial support from Consejo Nacional de Investigaciones Científicas y Técnicas (CONICET), Agencia Nacional de Promoción Científica y Tecnológica (ANPCyT), Agencia Córdoba Ciencia (ACC) and Secretaría de Ciencia y Técnica of Universidad Nacional de Río Cuarto (SECyT UNRC) all from Argentine, is gratefully acknowledged.

References

[1] D. R. Cardoso, S. H. Libardi, L. H. Skibsted. *Food Funct.* **3**, 487 (2012).
[2] N. T. Manojlovic, P. J. Vasiljevic, P. Z. Maskovic, M. Juskovic, G. Bogdanovic-Dusanovic. *Evid. Based Complement. Alternat. Med.* **2012**, 1 (2012).
[3] P. F. Heelis. *Chem. Soc. Rev.* **11**, 15 (1982).
[4] P. F. Heelis, F. Muller. in *Chemistry and Biochemistry of Flavoenzymes*, CRC Press, pp. 171–193 (1991).
[5] W. A. Massad, Y. Barbieri, M. Romero, N. A. Garcia. *Photochem. Photobiol.* **84**, 1201 (2008).
[6] W. A. Massad, S. Bertolotti, N. A. García. *Photochem. Photobiol.* **79**, 428 (2004).
[7] R. Sisodia, M. Geol, S. Verma, A. Rani, P. Dureja. *Nat. Prod. Res.* **27**, 2235 (2013).
[8] A. Güvenç, E. Küpeli Akkol, İ. Süntar, H. Keleş, S. Yıldız, İ. Çalış. *J. Ethnopharmacol.* **144**, 726 (2012).
[9] F. C. Odds. *Candida and Candidosis: A Review and Bibliography. 2nd Edition.* (Bailliere Tindall, London, 1988).
[10] U. Flückiger, O. Marchetti, J. Bille, P. Eggimann, S. Zimmerli, A. Imhof, J. Garbino, C. Ruef, D. Pittet, M. Täuber, others. *Swiss Med. Wkly* **136**, 447 (2006).
[11] J. A. Morris, A. Khettry, E. W. Seitz. *J. Am. Oil Chem. Soc.* **56**, 595 (1979).
[12] I. Stojanović, N. Radulović, V. Cvetković, T. Mitrović, S. Stamenković. *Facta Univ.-Ser. Phys. Chem. Technol.* **11**, 45 (2013).
[13] F. C. Odds, N. A. R. Gow, A. J. P. Brown. "Molecular principles of fungal pathogenesis," in J. Heitman, S. G. Filler, J. E. Edwards, A. P. Mitchell, (Eds.), pp. 305–319, ASM Press, Washington DC (2006).
[14] H.-Y. P. Chang, J. Chodosh. *Int. Ophthalmol. Clin.* **51**, 33 (2011).
[15] J. Natera, W. Massad, N. A. García. *Photochem. Photobiol. Sci.* **11**, 938 (2012).
[16] P. B. Merkel, D. R. Kearns. *J Am Chem Soc* **94**, 1029 (1972).
[17] R. Maurer, J. Vogel, S. Schneider. *Photochem. Photobiol.* **46**, 255 (1987).
[18] R. D. Scurlock, C. H. Evans, S. E. Braslavsky, K. Schaffner. *Photochem. Photobiol.* **58**, 106 (1993).
[19] J. W. Tukey. *Biometrics* **5**, 99 (1949).
[20] A. Pajares, M. Bregliani, W. Massad, J. Natera, C. Challier, L. Boiero, M. Montenegro, N. A. García. *J. Photochem. Photobiol. B* **135**, 48 (2014).
[21] H. Görner. *J. Photochem. Photobiol. B* **87**, 73 (2007).
[22] W. Lin, C. Lu, F. Du, Z. Shao, Z. Han, T. Tu, S. Yao, N. Lin. *Photochem. Photobiol. Sci.* **5**, 422 (2006).
[23] J. R. Lakowicz, K. A. P. Publishers. *Principles of Fluorescence Spectroscopy*, Kluwer Acadcemic/Plenum Publishers, 1999.
[24] C. M. Krishna, S. Uppuluri, P. Riesz, J. S. Zigler, D. Balasubramanian. *Photochem. Photobiol.* **54**, 51 (1991).
[25] A. Pajares, J. Gianotti, G. Stettler, S. Bertolotti, S. Criado, A. Posadaz, F. AmatGuerri, N. A. Garcia. *J. Photochem. Photobiol. Chem.* **139**, 199 (2001).
[26] E. Haggi, S. Bertolotti, S. Miskoski, F. Amat-Guerri, N. A. Garcia. *Can.J.Chem.* **80**, 62 (2002).
[27] I. Gutiérrez, S. Criado, S. Bertolotti, N. A. García. *J. Photochem. Photobiol. B* **62**, 133 (2001).
[28] E. J. Land, A. J. Swallow. *Biochemistry (Mosc.)* **8**, 2117 (1969).
[29] C. Y. Lu, W. Z. Lin, W. F. Wang, Z. H. Han, S. D. Yao, N. Y. Lin. *Phys. Chem. Chem. Phys.* **2**, 329 (2000).
[30] G. Rossbroich, N. A. Garcia, S. E. Braslavsky. *J. Photochem.* **31**, 37 (1985).
[31] I. Fridovich. *Photochem. Photobiol.* **28**, 733 (1978).
[32] I. B. Afanas'ev. *Superoxide Ion Chemistry and Biological Implications*, 1 edition, CRC Press, Boca Raton, Fla, 1989.
[33] D. R. Cardoso, K. Olsen, L. H. Skibsted. *J. Agric. Food Chem.* **55**, 6285 (2007).
[34] R. R. Yettella, D. B. Min. *Food Chem.* **118**, 35 (2010).
[35] N. K. Hall, T. M. Chapman, H. J. Kim, D. B. Min. *Food Chem.* **118**, 534 (2010).
[36] E. Haggi, N. Blasich, M. P. Montana, G. Ferrari, V. Mufioz, C. Challier, S. Criado, J. Natera, S. Miskoski, N. A. Garcia. *Curr. Top. Pept. Protein Res.* **14**, 55 (2013).
[37] R. T. Kashiwabuchi, F. R. S. Carvalho, Y. A. Khan, F. Hirai, M. S. Campos, P. J. McDonnell. *Graefes Arch. Clin. Exp. Ophthalmol.* **251**, 521 (2013).
[38] A. Sauer, V. Letscher-Bru, C. Speeg, D. Touboul, J. Colin, E. Candolfi, T. Bourcier. *Invest. Ophthalmol. Vis. Sci.* **51**, 3950 (2010).
[39] S. A. R. Martins, J. C. Combs, G. Noguera, W. Camacho, P. Wittmann, R. Walther, M. Cano, J. Dick, A. Behrens. *Invest. Ophthalmol. Vis. Sci.* **49**, 3402 (2008).
[40] M. P. Tampieri, R. Galuppi, F. Macchioni, M. S. Carelle, L. Falcioni, P. L. Cioni, I. Morelli. *Mycopathologia* **159**, 339 (2005).

[41] M. A. Slifkin. *Charge Transfer Interactions of Biomolecules*, Academic Press, 1971.
[42] Y. Barbieri, W. A. Massad, D. J. Díaz, J. Sanz, F. Amat-Guerri, N. A. Garcia. *Chemosphere* **73**, 564 (2008).
[43] F. Wilkinson, W. P. Helman, A. B. Ross. *J. Phys. Chem. Ref. Data* **24**, 663 (1995).
[44] S. Nonell, L. Moncayo, F. Trull, F. Amat-Guerri, E. A. Lissi, A. T. Soltermann, S. Criado, N. A. Garcia. *J. Photochem. Photobiol. B* **29**, 157 (1995).
[45] E. Haggi, S. Bertolotti, N. A. Garc¡a. *Chemosphere* **55**, 1501 (2004).
[46] R. Yin, T. Dai, P. Avci, A. E. S. Jorge, W. C. de Melo, D. Vecchio, Y.-Y. Huang, A. Gupta, M. R. Hamblin. *Curr. Opin. Pharmacol.* **13**, 731 (2013).
[47] J. W. Ferguson, J. F. Hatton, M. J. Gillespie. *J. Endod.* **28**, 68 (2002).